Structural Performance of Reinforced Strain Hardening Cementitious Composite Pipes during Cyclic Loading

Structural Performance of Reinforced Strain Hardening Cementitious Composite Pipes during Cyclic Loading

Jun Li[1, *], Yujuan Li[2, a], Jiao Guo[1, b], Meinan Wan[1, c] and Xun Dong[1, d]

[1]School of Architectural Engineering, Huanggang Normal University, Huangzhou, China
[2]Ezhou Transport Bureau, E-zhou, China

*Corresponding author e-mail: 373633802@qq.com, [a]273800525@qq.com, [b]303710257@qq.com, [c]310312817@qq.com, [d]352253040@qq.com

Abstract. Strain Hardening Cementitious Composites (SHCC) is a kind of micromechanically designed cement-based composite with ultra high tensile ductility. It is used to fabricate an innovative concrete pipe to improve the structural performance of concrete pipe. The failure processes of reinforced SHCC pipes (RSHCCP) in comparison to these of conventional reinforced cement mortar pipes (RMP) have been investigated under the Three-Edge Bearing Testing (TEBT). Results show that RSHCCP, RMP reveal flexural hardening phenomenon, and RSHCCP's hardening stage is first steep after slow, and has a large deformation, and others is more gently. During cyclic loading, the ring stiffness of pipes were constantly decreases, and the ring stiffness of RSHCCP at hardening stage decreases, is about 20% ~ 90% of the initial ring stiffness.

1. Introduction

The mechanical performance of SHCC is excellent, and the tensile strain is above 3%, processing strain hardening characteristics and multiple fine crack phenomenons [1], its good tensile performance will improve the bearing capacity and ductility of concrete structure. At present, SHCC has been applied in the reinforced concrete beam, wall, bridge and tunnel [2]. And the flexural capacity and ductility of steel reinforced SHCC (RSHCC) beam was superior to reinforced concrete (RC) beams, and reduced the reinforcement ratio, and presented multiple fine crack [3]. The bearing capacity and bending performance of SHCC/RC composite beam were significantly improved, and SHCC played the role of dispersing and inhibiting crack development [4, 5]. Cho [6] found that the stiffness and ultimate load of composite board had been improved through bending test of RSHCC composite panels.

The research of SHCC in beam and slab structure had been reported, whereas the ones in the pipe are still in its infancy. Haktanir [7], MacDonald [8] found that the strength and stiffness of steel fiber reinforced concrete (SFRC) pipe was similar to RC pipe, and the performance after cracked was improved. Peyvandi [9, 10] had an experimental research on polyvinyl alcohol (PVA) fiber reinforced concrete pipe, and found that PVA fiber played the role of reducing the reinforcement ratio and enhancing its structure performance significantly. Referring to the above research, the differences of structural performance under monotonous loading had been studied between RSHCCP and RMP [11],

and discovered that bearing capacity and deformation ability of RSHCCP was superior to RMP, and showed multiple fine crack phenomenon similar to SHCC under uniaxial tension. However, the analysis of failure process and ring stiffness is not enough. Therefore, the experimental research during cyclic loading on RSHCCP and RMP is adopted to discuss the failure process and ring stiffness, and to discuss its structure performance deeply.

2. Materials and methods

2.1. Raw materials and mix proportion

SHCC is often prepared with cement[1], fly ash[2], fine sand[3], fine PVA fibers[4] and other admixtures[5] without coarse aggregate [12]. So, pipes to study in this paper are not concrete. Hereinafter, steel reinforced SHCC pipes, steel reinforced cement mortar pipes are denoted as RSHCCP and RMP, respectively. Test pipes include RSHCCP and RMP. The raw materials and mix proportion can be found in Table 1. And the properties of PVA fiber are shown in Table 2.

Table 1. Mix proportion and reinforcement ratio.

	C	FA	S	W	WR	VMA	PVA
RSHCCP	1	2.0	1.36	0.93	0.018	0.00075	0.066
RMP	1	2.0	1.36	0.93	0.018	0.00075	—

Table 2. Properties of PVA fiber.

length	diameter	young's modulus	relative density	elongation	Tensile Strength
12mm	39μm	42.8GPa	1300kg/m3	7%	1620MPa

One circular reinforcement cage with a reinforcement area of 2.5cm^2 per linear meter of pipe wall was embedded into pipes. The reinforcement cage was welded using ribbed steel rebar with a young's modulus of 210GPa and yield strength of 600MPa. The diameters of circumferential reinforcement and longitudinal reinforcement were 4mm and 5mm, respectively.

2.2. Preparation of specimens

The preparation progress is shown in Fig. 1.

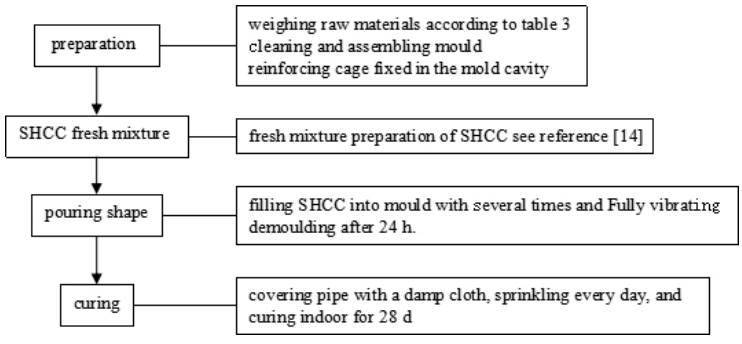

Figure 1. Preparation progress.

[1] Huaxin Cement Co. Ltd., Hubei Province, China.
[2] Huaneng Yangluo Power Plant, Hubei Province, China.
[3] Shuangxin mineral powder Co. Ltd., Hubei Province, China
[4] Kuraray Co. Ltd. Japan.
[5] Viscosity modifier agent by BASF in China, and water reducing agent by GRACE Shanghai Branch, China.

2.3. Methods of three-edge bearing test (TEBT)

In AS 4139-2003 [13] and GB/T 16752-2006 [14], TEBT is used to monitor the bearing and deformation capacity of pipe. Experimental setup for TEBT is shown in Fig. 2, and experiments would be implemented on Instron 5882 electronic universal material testing machine. From top to bottom in turn to load sensor, steel beam, rubber pad, specimen, an LVDT, the wireless strain acquisition node, plastic bearings and steel plate, etc. Two bearers made of high-strength engineering plastic had cross-sectional dimension of 48mm × 48mm and length of 380mm. They were firmly fixed in a 20mm thick steel plate, which was fixed on the bottom plate of Instron 5882 testing equipment using six bolts. The surface of a Type 6.3 hot-rolled channel steel as the loading beam in contact with the pipe was faced with 25mm thick hard rubber packing. According to the standard, the distance between two plastic bearing is $D/12$.

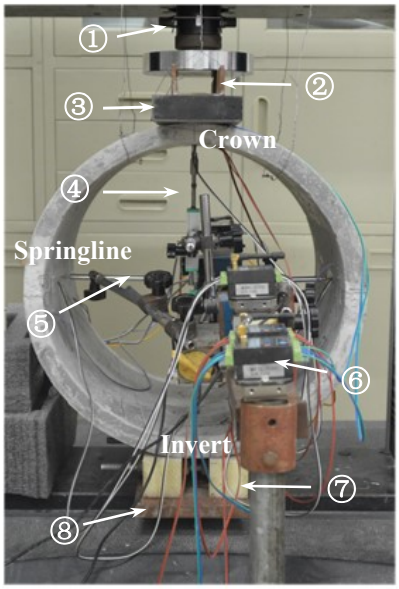

1. Load sensor
2. Steel beam
3. Rubber pad
4. LVDT
5. LVDT
6. Wireless strain acquisition
7. Plastic bearings
8. Steel plate

Figure 2. Setup for TEBT on pipes.

Fig. 3 showed loading steps of TEBT during cyclic loading, which includes 10 and 6 load peaks for RSHCCP and RMP, respectively. For the pipes, the difference between adjacent load peaks is 3.13kN/m for RSHCCP and 1.56kN/m for RMP. Test environment was at a temperature of 25℃ and at 70% RH.

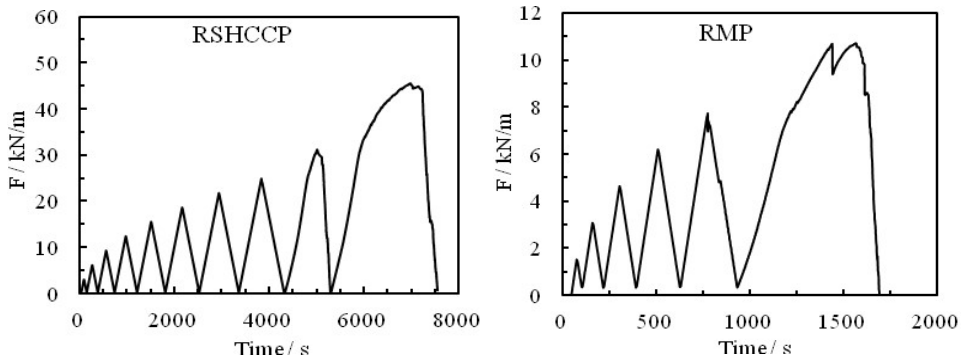

Figure 3. Test process for cyclic loading.

2.4. Deflection measurement for pipes under TEBT

Four LVDTs located at the center, respectively to measure the deflection of crown, invert and springlines. As shown in Fig. 2, LVDTs were positioned against the inner surface of the pipe crown, the left springline, the pipe invert and the right springline, respectively. They were attached to a support steel beam, which was laid along the axis of the pipe and fixed on the floor. A data logger was used to collect deflections.

2.5. Calculation method of ring stiffness pipes

The calculation formula for ring stiffness at elastic stage can be shown as follow:

$$SN_i = \frac{0.149}{8} \cdot \frac{F_i}{\Delta_i} \times 10^9 \tag{1}$$

where SN_i is the ring stiffness, and F_i , Δ_i are the peak load and recoverable deflection corresponding to SN_i .

3. Results and discussions

3.1. Failure process analysis during loading

The load and deflection relation curve of RSHCCP and RMP at crown under TEBT during cyclic load were shown in Fig. 4. Results show that the deflection can recover after unloading unless the load exceeded the elastic limit, which were 12.3kN/m and 6.3kN/m for RSHCCP and RMP, respectively. Then increasing the load, RSHCCP, RMP revealed flexural hardening phenomenon to different degrees, as shown in Fig.4, the curve of RMP emerged larger fluctuations whereas the curves of RSHCCP were smooth. That's because, the failure of RMP caused by a single crack, the load would decrease if the crack propagated. However, RSHCCP appeared multiple crack phenomenons, and the influence on the propagation of single crack was weakened.

The envelopes of load and deflection curve under cyclic loading could be found in Fig.4, and the relationship of load and deflection under monotonic loading was shown in Fig.5. Compared with Fig.4 and Fig.5, it was shown that the shapes of envelopes was consistent with load and deflection curve under monotonic loading and the deflections corresponding to the failure loads had little difference for them. However, the failure loads during cyclic loading were slightly lower than the ones during monotonic loading. For RSHCCP and RMP, the failure loads during monotonic loading were 51.3kN/m and 15.0kN/m, respectively. Whereas, the failure loads during monotonic loading were about 45kN/m and 10.5kN/m, respectively, the phenomenon maybe due to the damage accumulating as the peak load increasing under cyclic loading.

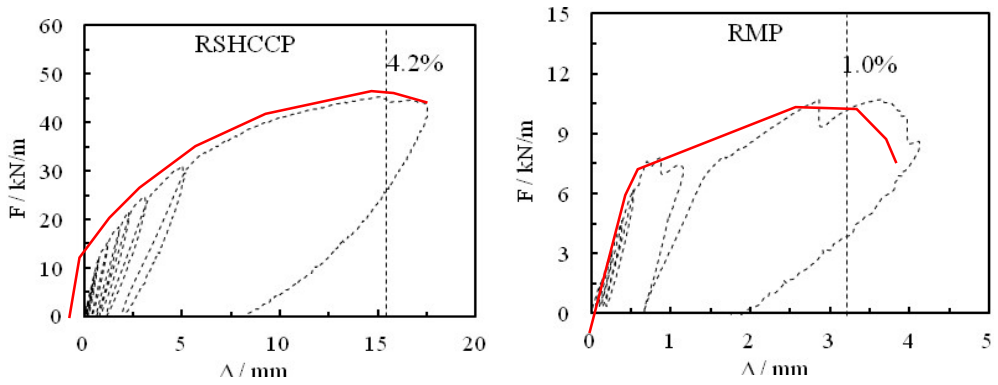

Figure 4. Relationship between load and deflection curve during cyclic loading.

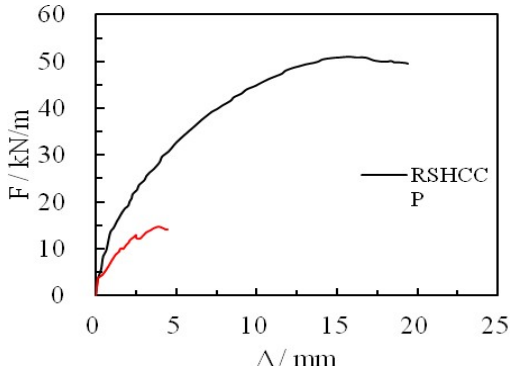

Figure 5. Relationship between load and deflection curve during monotonic loading.

According to the curves of load and deflection during cyclic and monotonic loading, it was believed that the failure process of RSHCCP and RMP included two stages under TEBT: (1) Elastic stage: it existed a direct proportion relationship between load with deflection at crown, and the deflection was recoverable after unloading. The proportional limit for RSHCCP was slightly higher than RMP. It showed that the property was mainly related to the matrix materials at elastic stage. (2) Hardening stage: both of curves entered the flexural hardening stage after elastic stage. At hardening stage, the curve was long and first steep after slow for RSHCCP, while it was much more gently for RMP.

Fig.6 showed a part of loading enlarge figure for RSHCCP. It displayed that the slope of unloading curve was below loading curve in a cycle. The curve of loading and unloading forms a hysteretic loop. Once the load exceeded the previous peak load, the curve would continue developing as the trend of monotonic loading. The figure also presented that the irreversible deformation of RSHCCP heightens gradually as the increasing peak load. Immediately, the slope of curve reduced and damage increased. Other pipes existed the same phenomenon.

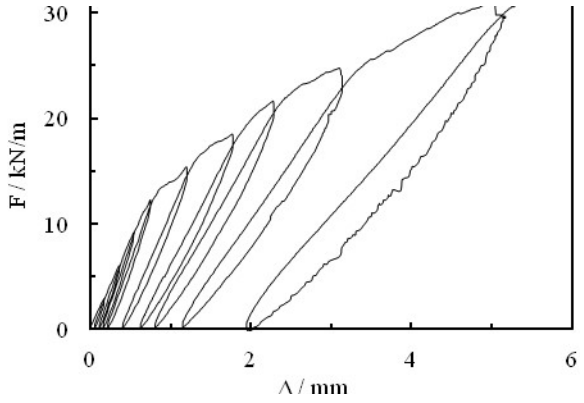

Figure 6. Part of loading enlarge figure for RSHCCP during cyclic loading.

3.2. Discussion of the semi-rigid pipe Results of ring stiffness calculation

Equ.(1) only applied to elastic stage, and the ring stiffness calculation needed a linear relationship while calculating the ring stiffness. In Fig.5, the inflection point appeared on the loading curves at hardening stage, therefore, the unloading curve was selected to calculate the ring stiffness. As shown in Fig.7, F_i is the load at unloading point, Δ_i is the recoverable deflection after unloading.

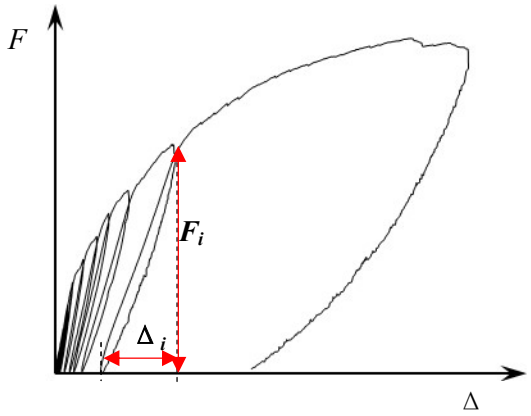

Figure 7. Accessor methods for ring stiffness calculation.

Table 3 listed the values of F_i, Δ_i and SN_i during cyclic loading for RSHCCP and RMP. The results showed that the initial ring stiffness for RSHCCP was greater. During cyclic loading, the ring stiffness of RSHCCP remained unchanged and gradually decreaseed with the increasing load. Whereas, RMP's stayed the same then decreased rapidly until failure stage.

Table 3. Changes of ring stiffness for pipes.

RSHCCP	F_i	2.93	6.05	9.19	12.31	15.44	18.56	21.69	24.78	31.06	43.75
	Δ_i	0.11	0.24	0.37	0.53	0.79	1.14	1.46	1.95	2.93	8.65
	SN_i	477	472	462	435	365	304	276	236	198	94
RMP	F_i	1.20	2.76	4.33	5.89	7.06	8.47	-	-	-	-
	Δ_i	0.06	0.16	0.24	0.33	0.41	2.54	-	-	-	-
	SN_i	371	330	336	335	320	62	-	-	-	-

Note: In the table, the unit for F_i is kN/m, the unit for Δ_i is mm, the unit for SN_i is kPa.

Fig.8 shown the ring stiffness curve, whose abscissa axis is $F_i/(F_i)_{\max}$ and vertical axis is SN_i. It characterizes the change law of ring stiffness, and it could be found that the ring stiffness curves could be divided into two parts. For RSHCCP, if $F_i/(F_i)_{\max}$ was less than 0.3, it stayed at elastic stage, and the ring stiffness remained unchanged; Once $F_i/(F_i)_{\max}$ exceeded 0.3, the ring stiffness decreased gradually, which was about 20% ~ 90% of the initial ring stiffness, and the final ring stiffness was 94kPa. So the critical value of $F_i/(F_i)_{\max}$ for RSHCCP is 0.3. Whereas the critical value of $F_i/(F_i)_{\max}$ for RMP were 0.8, respectively. Namely if $F_i/(F_i)_{\max}$ for RMP was below 0.8, the ring stiffness stayed the same; Once $F_i/(F_i)_{\max}$ for RMP was greater than 0.8, the ring stiffness decreased rapidly as the increasing load. Finally, the ring stiffness corresponding to the failure load was 25% of the initial ring stiffness for SHCCP, whereas for RMP it was less than 20% of the initial ring stiffness. Meanwhile, the ring stiffness for RSHCCP reduced slower than RMP, and lasted for a long time, it was related to the fine and multiple crack.

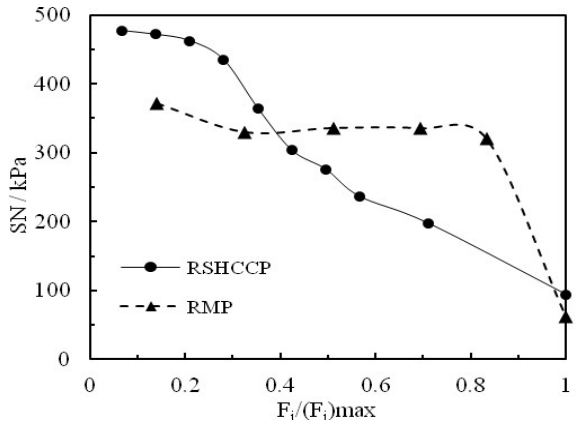

Figure 8. The change of ring stiffness.

4. Conclusion

This paper explores the structural performance of RSHCCP and RMP under TEBT during cyclic loading and monotonic loading. RSHCCP has high loading-carrying capacity and ultra-high deformation. Above all, the following conclusion can be drawn:

(1) The curve of load and deflection for RSHCCP and RMP include elastic stage and hardening stage. Whereas hardening stage of RSHCCP is first steep after slow, and has a large deformation, and others is more gently.

(2) During cyclic loading, the ring stiffness of pipes was constantly decreases, damage accumulates, and failure load reduces. In the hardening stage ring stiffness of RSHCCP decreases, is about 20% ~ 90% of the initial ring stiffness.

Acknowledgements

This work was financially supported by Youth Talent Project of Hubei Provincial Department of Education (30002/03201810902), and thanks for the experimental guidance and support from the Department of Mechanics of Wuhan University of Technology.

References

[1] J. Li, M.Q. Sun, Y.J. Wang, X.Y. Zhang, Preparation and tension performance of strain hardening cement-based composite, J. Funct Mater, 45 (2014) 117-121.

[2] M. Kunieda, K. Rokugo. Recent progress on HPFRCC in Japan required performance and applications, J. ADV Concr Technol, 4 (2006) 19-33.

[3] Q.H. Li, S.L. Xu. Experimental investigation and analysis on flexural performance of functionally graded composite beam crack-controlled by ultrahigh toughness cementitious composites, Sci, 52 (2009) 1648-1664.

[4] Y.K. Yun, Y.L. Bang, J.W. Bang, Flexural performance of reinforced concrete beams strengthened with strain-hardening cementitious composite and high strength reinforcing steel bar, Composites Part B. 56 (2014) 512-519.

[5] A.P. Lampropoulos, S.A. Paschalis, O.T. Tsioulou, Strengthening of reinforced concrete beams using ultra high performance fibre reinforced concrete (UHPFRC), Eng Struct, 106 (2016) 370-384.

[6] C.G. Cho, A.J. Kappos, H.J. Moon, Experiments and Failure Analysis of SHCC and Reinforced Concrete Composite Slabs, Eng Fail Anal, 56 (2015) 320-331.

[7] T. Haktanir, K. Ari, F. Altun, A comparative experimental investigation of concrete, reinforced-concrete and steel-fibre concrete pipes under three-edge-bearing test, Constr Build Mater, 21 (2007) 1702-1708.

[8] C. MacDonald, J. Trangsrud, Steel fiber product introduction through pre-cast reinforced

concrete pipe, ACI Special Publication, 222 (2004) 185-99.
[9] A. Peyvandi, P. Soroushian, S. Jahangirnejad, Enhancement of the structural efficiency and performance of concrete pipes through fiber reinforcement, Constr Build Mater, 45 (2013) 36–44.
[10] A. Peyvandi, P. Soroushian, S. Jahangirnejad, Structural design methodologies for concrete pipes with steel and synthetic fiber reinforcement,. ACI Struct J, 111 (2014) 83-92.
[11] J. Li, M.Q. Sun, J.H. Hu, Structural performance of reinforced strain hardening cementitious composite pipes during monotonic loading, Constr Build Mater, 114 (2016) 794-804.
[12] Y. Park, A. Abolmaali, J. Beakley, Thin-walled flexible concrete pipes with synthetic fibers and reduced traditional steel cage, Eng Struct, 100 (2015) 731-741.
[13] AS4139-2003, Fiber-Reinforced Concrete Pipe and Fitting (2003).
[14] GB/T16752-2006, Test Methods of Concrete and Reinforced Concrete Drainage and Sewer Pipes (2006).